

Classification of dark energy models in the (w_0, w_a) plane

V. Barger¹, E. Guarnaccia² and D. Marfatia²

¹*Department of Physics, University of Wisconsin, Madison, WI 53706*

²*Department of Physics and Astronomy, University of Kansas, Lawrence, KS 66045*

Abstract

We classify dark energy models in a plane of observables that correspond to the common parameterization of a non-constant equation of state, $w(a) = w_0 + w_a(1 - a)$, where a is the scale factor of the universe. The models fall into four classes and only two of these classes have a region of overlap in the observable plane. We perform a joint analysis of all Type Ia supernova (SNIa) data compiled by the High-Z SN Search Team (HZT) and the Supernova Legacy Survey (SNLS) and find that no class of models is excluded by current SNIa data. However, an analysis of large scale structure, Ly α forest and bias constraints from SDSS, the Gold SNIa data and WMAP data indicates that non-phantom barotropic models with a positive sound speed are excluded at the 95% C. L.

Abundant cosmological data indicate that the expansion of the universe has changed from a decelerating phase to an accelerating phase in the last few billion years. This is generally attributed to the recent dominance of an energy component with negative pressure called dark energy¹. For reviews see Ref. [2].

Among candidates for dark energy are the cosmological constant Λ proposed by Einstein and a dynamical scalar field such as quintessence [3, 4, 5]. The cosmological constant arises in particle physics as vacuum energy with constant energy density ρ , constant pressure p and equation of state $w \equiv p/\rho = -1$. A cosmological constant is troublesome from the particle physics standpoint because the cosmologically measured value of $\rho_\Lambda^{1/4}$ is found to be about $(0.7\rho_c)^{1/4} \simeq 0.002$ eV, where ρ_c is the critical density for which the universe is flat. Quantum field theory, however, suggests a value at least 15 orders of magnitude larger under the assumption that the Standard Model is an effective theory valid below 1 TeV. For the vacuum energy to be renormalized to 0.002 eV, a fine tuning in the energy density at the level 60 decimal places is required. See Ref. [6] for a review of the cosmological constant problem. Compounding this, is the cosmic coincidence problem which seeks an explanation for why the dark matter and vacuum energy densities are comparable today although their ratio scales as $1/a^3$, where $a = 1/(1+z)$ in terms of redshift z [2]. Quintessence is not a solution, but provides a phenomenological explanation for these problems. It is a time-varying field with $w(a) > -1$ and is usually represented by a very light scalar field rolling down a potential. The potential and field values are chosen so that the energy density in quintessence dominates the dark matter density only recently and takes on the measured value. This picture has been generalized to schemes with $w < -1$ called phantom dark energy and to dark energy as a barotropic fluid with $w = f(\rho)/\rho$. In what follows, we consider phantom models, barotropic fluid models of dark energy and two classes of quintessence models.

Recently, in a sequence of papers [7, 8, 9], models of dark energy have been divided into categories depending on their equation of state, w , and its derivative with respect to the logarithm of the scale factor, $w' \equiv \frac{dw}{d\ln(a)}$; since $H^{-1} = \frac{dt}{d\ln(a)}$, w' is the time derivative of w in units of Hubble time. It was pointed out that different classes of models evolve in different regions of the $w - w'$ plane².

Building on this work, we classify models of dark energy in a parameter space of observables. It has been argued in Ref. [11], that given the sensitivities of future cosmological experiments, one can realistically expect to constrain at most two parameters related to the equation of state.

¹Modifications to the Friedman-Robertson-Walker equation can also provide an explanation for the current accelerated expansion such as in Cardassian models [1] which do not have exotic forms of energy or a vacuum contribution. We do not consider such models here.

²Equivalently, different dark energy models evolve in different regions of statefinder planes [10]; the statefinder diagnostic, defined in terms of the second and third time derivatives of a , is directly related to w and w' .

Specifically, we use the standard parameterization of dark energy evolution in terms of the equation of state and its derivative with respect to z at the present time [12]:

$$w(z) = w_0 + w_a \frac{z}{1+z} \quad (1)$$

with

$$w_a = \left. \frac{dw}{dz} \right|_{z=0} = -2w' \Big|_{z=1}. \quad (2)$$

Note the relationship between w_a and the value of w' at $z = 1$, the epoch when the dark energy contribution to the expansion rate is expected to increase in importance³. We classify models in the $w_0 - w_a$ plane. The primary advantage of this parameterization is that since the dark energy density evolves according to

$$\rho(z) = \rho(0)(1+z)^{3(1+w_0+w_a)} e^{-3w_a \frac{z}{1+z}}, \quad (3)$$

it is well-behaved from high redshifts until today. Note that for dark energy to be subdominant at early times, $w_0 + w_a < 0$. We do not impose the latter restriction since the parameterization of Eq. (1), though well-behaved at high redshift, may be inapplicable there.

The previously popular linear parameterization $w(z) = w_0 + w_1 z$ [16] diverges at high redshift and consequently yields artificially strong constraints on w_1 in analyses involving data at high redshifts such as CMB data. Since Eq. (1) is often used in the analysis of data, our classification will enable a direct comparison between the results of such analyses and the theoretical space of models.

The categorization we develop is analogous to that of inflationary models where models populate regions in a plane defined by the spectral index of scalar perturbations, n_s , and the relative normalization of the tensor and scalar spectra, R [17], or in a plane of horizon-flow parameters [18].

Dark energy models:

Here, we briefly review the models under consideration, define the regions they occupy in the $w - w'$ plane and classify them in the $w_0 - w_a$ plane.

We first consider models which obey the null energy condition, $w \geq -1$, and then consider phantom models with $w < -1$.

Thawing models

The nomenclature, “thawing” models, was coined in Ref. [7] to describe a scalar field whose equation of state increases (thaws out) from $w \simeq -1$ as the scalar rolls down towards the minimum

³In Refs. [13, 14], the transition from matter domination to dark energy domination is found to occur at $z \simeq 0.5$. For a recent discussion of the low redshift evolution of the dark energy density see Ref. [15].

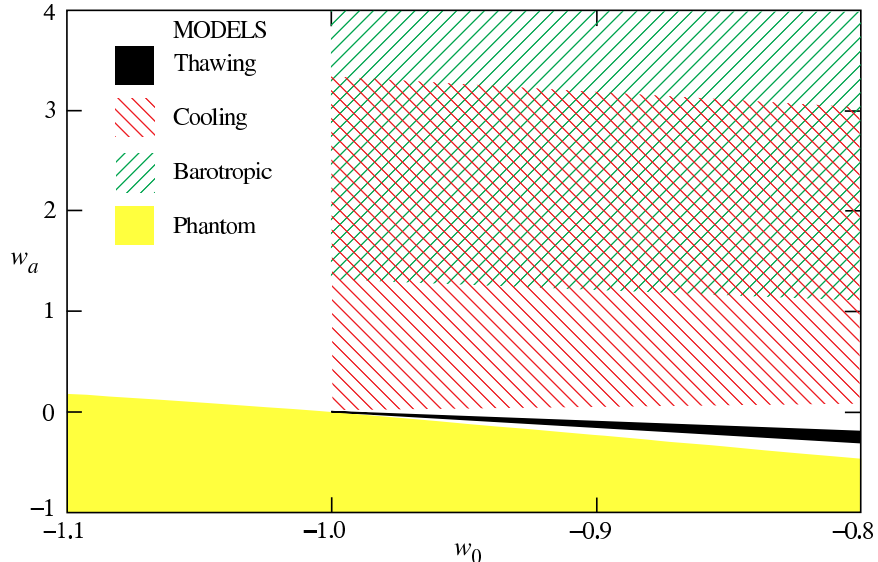


Figure 1: Classification of the four types of models in the (w_0, w_a) plane.

of its potential. Potentials of the form ϕ^n (with $n > 0$) and $e^{-\phi}$ are typical of these models. Particle-physics models involving axions [19], pseudo Nambu-Goldstone bosons [4], moduli or dilatons [20] often have such potentials. They are found to satisfy [7]

$$1 + w < w' < 3(1 + w). \quad (4)$$

It is natural to impose this constraint at the epoch when dark energy starts becoming important, *i.e.*, $z = 1$. With $w(1) = w_0 + w_a/2$ and $w'|_{z=1} = -w_a/2$, we find

$$-\frac{3}{2}(1 + w_0) < w_a < -(1 + w_0). \quad (5)$$

Thawing models occupy the dark-shaded triangular wedge in Fig. 1.

Cooling models

In these models, initially, $w > -1$ and w decreases as the scalar rolls down the potential, which is typically of the form ϕ^{-n} or $\phi^{-n}e^{\phi^2}$ (with $n > 0$). The tracker models of Ref. [21] adopt such potentials. Such forms of the potential also arise in models of dynamical supersymmetry breaking [22] and supergravity [23]. These models lie in a region of the $w - w'$ plane defined by [7, 8, 9]

$$-3(1 - w)(1 + w) < w' < 0.2w(1 + w). \quad (6)$$

By requiring that $w(1)$ obey the above inequality, we obtain the region with red slant hatches (with negative slope) in Fig. 1. As shown in Ref. [9], k -essence models [24] with a non-linear kinetic term also fall within the class of cooling models.

Note that the “freezing” models of Ref. [7] are a special case corresponding to the situation in which the potential has a minimum at $\phi = \infty$. For freezing models,

$$3w(1+w) < w' < 0.2w(1+w). \quad (7)$$

Barotropic fluids

A barotropic fluid is one for which the density depends only on the pressure. Supposing that dark energy is a barotropic fluid with $p = f(\rho)$ leads to a class of models that contains as special cases the generalized Chaplygin gas [25] for which $f(\rho) = -A/\rho^\alpha$ with $\alpha > -1$ and the original Chaplygin gas model with $\alpha = 1$ [26]. While the models of Refs. [25, 26] were proposed to unify dark matter and dark energy, subsequent work addressed the possibility of Chaplygin gas models as being models of dark energy alone [27]. Barotropic fluid models arise in string theories [28] in which *e.g.* the Chaplygin gas corresponds to a gas of d -branes in a $d + 2$ spacetime [29].

Non-phantom barotropic models were found to satisfy [8]

$$w' < 3w(1+w) \quad (8)$$

under the assumption that $c_s^2 \equiv dp/d\rho > 0$ so that perturbation growth is stable.

The region with green slant hatches (with positive slope) in Fig. 1 depicts barotropic fluids. This region partially overlaps with that for cooling models.

Comparing Eq. (7) with Eq. (8), we see that freezing models and barotropic fluids have nonoverlapping regions with a common boundary in the $w - w'$ plane. In the observable $w_0 - w_a$ plane, freezing models occupy the region with red slant hatches (with negative slope) below the cross hatched region (non-overlapping with the region occupied by barotropic fluid models). See Fig. 1.

Phantom models

Finally, we consider phantom models for which $w < -1$. It was shown in Ref. [9] that for the prototypical phantom (*i.e.* a ghost with a negative kinetic term) model [30],

$$3(1-w)(1+w) < w' < 3w(1-w)(1+w). \quad (9)$$

Such models populate the light yellow shaded region in Fig. 1.

Note that not all models that violate the null energy condition require the scalar to be a phantom. Demonstrations of the violation of the null energy condition have been made in models of vacuum metamorphosis [31], climbing scalar fields [32], and the braneworld [33] without the introduction of negative energies or negative norm states.

We caution against interpreting this classification as being comprehensive. For example, dark energy with an oscillating equation of state [34] can rarely be realized in a potential formulation.

(An example of oscillating dark energy from a quite complicated potential can be found in Ref. [35]). Thus, oscillating dark energy as a class of models falls outside the realm of our classification. Similarly, we have not attempted to include neutrino dark energy [36] or dark energy with generalized equations of state [37] in the classification.

When viewed in conjunction with data, our classification is intended to provide guidance as to what kinds of schemes are preferred by data. It is necessary that a cosmological constant $(w_0, w_a) = (-1, 0)$, be excluded by data to distinguish between thawing, cooling and phantom models because these models have a cosmological constant as a limiting case. This is in contrast to barotropic fluids with a positive sound speed.

Current status:

Having defined the regions that the four different types of models occupy in the $w_0 - w_a$ plane, we now examine if current data are able to discriminate between these classes.

We perform a joint analysis of SNIa data compiled by the High-Z SN Search Team (HZT) and the Supernova Legacy Survey (SNLS). We include the Gold and Silver datasets of Ref. [13], the 4 SN of Ref. [14], and the SNLS dataset [38] assuming a flat universe with $0.2 \leq \Omega_m \leq 0.4$ and $0.5 \leq h \leq 0.9$. We have removed the SN common to both surveys from the SNLS dataset which results in a full dataset of 266 SN. Our joint analysis is implemented as follows. The statistical significance of a cosmology is determined in terms of $\chi^2 = \chi_{\text{HZT}}^2 + \chi_{\text{SNLS}}^2$, with

$$\chi_{\text{HZT}}^2 = \sum_{i=1}^{188} \frac{(\mu_i^{\text{obs}} - 5 \log_{10} d_L(z_i; \Omega_m, h, w_0, w_a) - M_1)^2}{\sigma_i^2}, \quad (10)$$

$$\chi_{\text{SNLS}}^2 = \sum_{i=1}^{78} \frac{(\mu_i^{\text{obs}} - 5 \log_{10} d_L(z_i; \Omega_m, h, w_0, w_a) - M_2)^2}{\sigma_{\mu_i}^2 + \sigma_{\text{int}}^2}. \quad (11)$$

where μ_i^{obs} is the distance modulus at redshift z_i , d_L is the luminosity distance (in units of 10 pc), σ_i is the total uncertainty in the distance modulus, $\sigma_{\mu_i}^2$ is the measurement variance and σ_{int} is the intrinsic dispersion of SN absolute magnitudes. M_1 and M_2 are nuisance parameters that are marginalized over in the fit. They correspond to analysis-dependent global unknown constants in the definition of distances. M_1 and M_2 are analogous to absolute magnitudes if observational data are provided as apparent magnitudes.

Note that SNLS provides the apparent magnitudes, the stretch factor used to calibrate them, and the rest frame color factor that measures host galaxy dust extinction. We have chosen to use the derived μ values instead for two reasons: (1) it is not possible to perform an analysis at the same level of sophistication for the HZT data since the High-Z SN Search Team provides only the distance modulus (*i.e.*, after corrections have been made to the apparent magnitude $m(z)$), and (2) it would be overkill considering that current SN data are not very constraining in the (w_0, w_a)

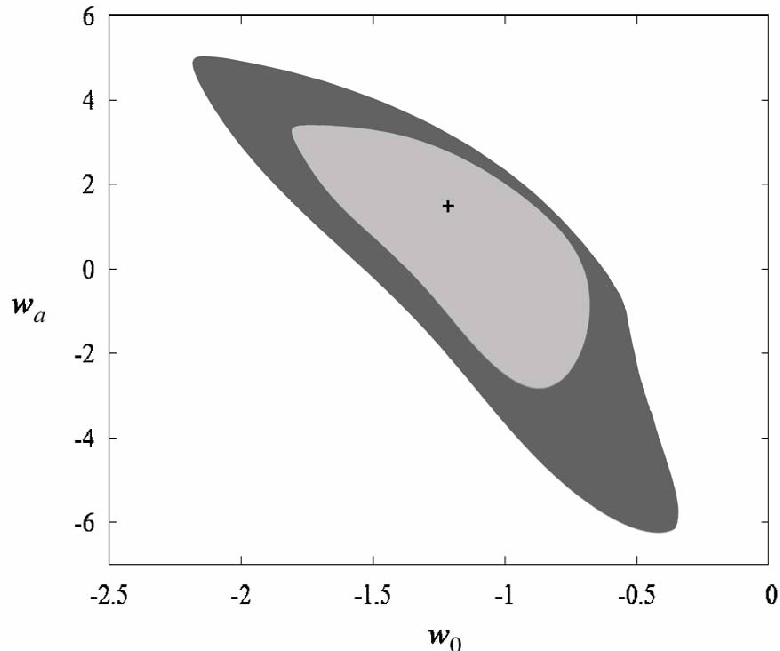


Figure 2: 68% C. L. and 95% C. L. allowed regions from a combined analysis of the HZT and SNLS SNIa data. The crosshair marks the best-fit point $(w_0, w_a) = (-1.2, 1.5)$. No class of dark energy model is excluded.

plane.

Reference [38] finds $\sigma_{int} = 0.13 \pm 0.02$. To be conservative in our combined analysis we choose $\sigma_{int} = 0.15$. We emphasize that our approximate analysis of SNLS data alone yields good agreement with that of the more accurate analysis of Ref. [38] implemented in Ref. [39]. Gravitational lensing bias could be reduced by use of the flux-averaging procedure of Ref. [40].

In Fig. 2 we display the 68% and 95% C. L. allowed regions obtained in our analysis. We immediately conclude that all classes of dark energy models are comfortably allowed by current SN data. In Fig. 3 we overlay the results of an analysis of large scale structure, Ly α forest and bias constraints from SDSS, the Gold SNIa data and WMAP data on the plane of classification. The 68% and 95% C. L. allowed regions have been adapted from Fig. 9 of Ref. [41] after accounting for the fact that our w_a corresponds to $-w_1$ in Ref. [41].

It appears that current data exclude non-phantom barotropic models with a positive sound speed at the 95% C. L. Also, among cooling models, freezing models appear to be favored. However, it may be too soon to draw these conclusions with confidence because the analysis of several correlated datasets has led to these results. It will be more convincing if the same conclusions can be made from an analysis of fewer distinct but larger datasets. For a recent assessment of the abilities of

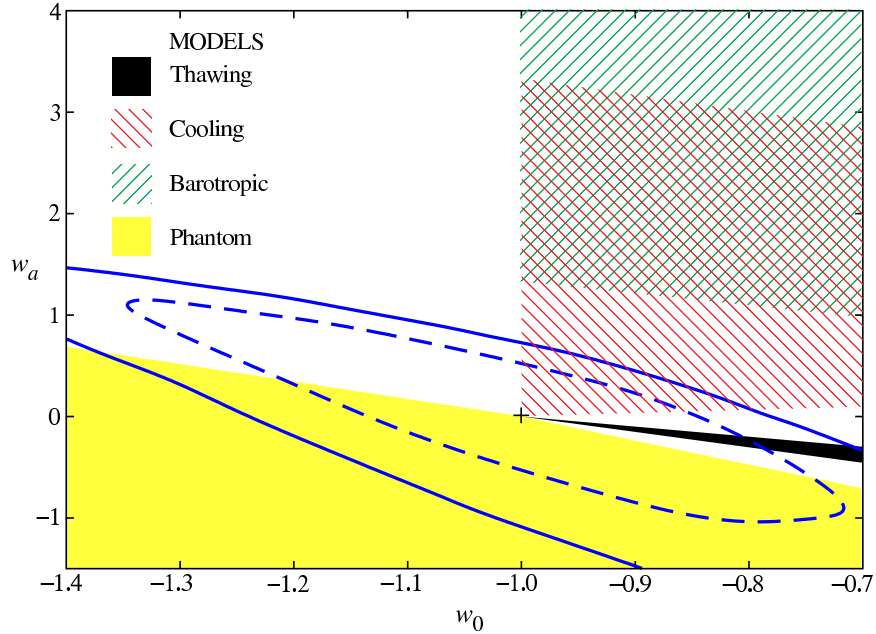


Figure 3: 68% C. L. and 95% C. L. allowed regions from an analysis of large scale structure, Ly α forest and bias constraints from SDSS, the Gold SNIa data and WMAP data. The crosshair marks the best-fit point $(w_0, w_a) = (-1, 0)$, which corresponds to a cosmological constant. Non-phantom barotropic models are excluded at the 95% C.L. (Adapted from Fig. 9 of Ref. [41]).

future dark energy surveys to discover the time evolution of w see Ref. [42].

Acknowledgments:

We thank P. Astier and Y. Wang for helpful communications. This research was supported by the U.S. Department of Energy under Grant No. DE-FG02-95ER40896, by the NSF under CAREER Award No. PHY-0544278 and Grant No. EPS-0236913, by the State of Kansas through the Kansas Technology Enterprise Corporation and by the Wisconsin Alumni Research Foundation.

References

- [1] K. Freese and M. Lewis, Phys. Lett. B **540**, 1 (2002) [arXiv:astro-ph/0201229].
- [2] P. J. E. Peebles and B. Ratra, Rev. Mod. Phys. **75**, 559 (2003) [arXiv:astro-ph/0207347]; T. Padmanabhan, Phys. Rept. **380**, 235 (2003) [arXiv:hep-th/0212290].
- [3] P. J. E. Peebles and B. Ratra, Astrophys. J. **325**, L17 (1988); B. Ratra and P. J. E. Peebles, Phys. Rev. D **37**, 3406 (1988); C. Wetterich, Nucl. Phys. B **302**, 668 (1988);
- [4] J. A. Frieman, C. T. Hill, A. Stebbins and I. Waga, Phys. Rev. Lett. **75**, 2077 (1995) [arXiv:astro-ph/9505060];
- [5] K. Coble, S. Dodelson and J. A. Frieman, Phys. Rev. D **55**, 1851 (1997) [arXiv:astro-ph/9608122]; R. R. Caldwell, R. Dave and P. J. Steinhardt, Phys. Rev. Lett. **80**, 1582 (1998) [arXiv:astro-ph/9708069].
- [6] S. Weinberg, Rev. Mod. Phys. **61**, 1 (1989).
- [7] R. R. Caldwell and E. V. Linder, Phys. Rev. Lett. **95**, 141301 (2005) [arXiv:astro-ph/0505494].
- [8] R. J. Scherrer, arXiv:astro-ph/0509890.
- [9] T. Chiba, arXiv:astro-ph/0510598.
- [10] V. Sahni, T. D. Saini, A. A. Starobinsky and U. Alam, JETP Lett. **77**, 201 (2003) [Pisma Zh. Eksp. Teor. Fiz. **77**, 249 (2003)] [arXiv:astro-ph/0201498]; U. Alam, V. Sahni, T. D. Saini and A. A. Starobinsky, Mon. Not. Roy. Astron. Soc. **344**, 1057 (2003) [arXiv:astro-ph/0303009].
- [11] E. V. Linder and D. Huterer, Phys. Rev. D **72**, 043509 (2005) [arXiv:astro-ph/0505330].
- [12] M. Chevallier and D. Polarski, Int. J. Mod. Phys. D **10**, 213 (2001) [arXiv:gr-qc/0009008]; E. V. Linder, Phys. Rev. Lett. **90**, 091301 (2003) [arXiv:astro-ph/0208512].
- [13] A. G. Riess *et al.* [Supernova Search Team Collaboration], Astrophys. J. **607**, 665 (2004) [arXiv:astro-ph/0402512].
- [14] A. Clocchiatti *et al.* [the High-Z SN Search Collaboration], arXiv:astro-ph/0510155.
- [15] H. K. Jassal, J. S. Bagla and T. Padmanabhan, Phys. Rev. D **72**, 103503 (2005) [arXiv:astro-ph/0506748].

- [16] I. Maor, R. Brustein and P. J. Steinhardt, Phys. Rev. Lett. **86**, 6 (2001) [Erratum-ibid. **87**, 049901 (2001)] [arXiv:astro-ph/0007297]; J. Weller and A. Albrecht, Phys. Rev. Lett. **86**, 1939 (2001) [arXiv:astro-ph/0008314]; V. D. Barger and D. Marfatia, Phys. Lett. B **498**, 67 (2001) [arXiv:astro-ph/0009256].
- [17] S. Dodelson, W. H. Kinney and E. W. Kolb, Phys. Rev. D **56**, 3207 (1997) [arXiv:astro-ph/9702166].
- [18] V. Barger, H. S. Lee and D. Marfatia, Phys. Lett. B **565**, 33 (2003) [arXiv:hep-ph/0302150].
- [19] P. Q. Hung, arXiv:hep-ph/0512282.
- [20] T. Barreiro, E. J. Copeland and N. J. Nunes, Phys. Rev. D **61**, 127301 (2000) [arXiv:astro-ph/9910214].
- [21] I. Zlatev, L. M. Wang and P. J. Steinhardt, Phys. Rev. Lett. **82**, 896 (1999) [arXiv:astro-ph/9807002].
- [22] P. Binetruy, Phys. Rev. D **60**, 063502 (1999) [arXiv:hep-ph/9810553]; A. Masiero, M. Pietroni and F. Rosati, Phys. Rev. D **61**, 023504 (2000) [arXiv:hep-ph/9905346].
- [23] P. Brax and J. Martin, Phys. Lett. B **468**, 40 (1999) [arXiv:astro-ph/9905040]; E. J. Copeland, N. J. Nunes and F. Rosati, Phys. Rev. D **62**, 123503 (2000) [arXiv:hep-ph/0005222].
- [24] C. Armendariz-Picon, V. Mukhanov and P. J. Steinhardt, Phys. Rev. Lett. **85**, 4438 (2000) [arXiv:astro-ph/0004134].
- [25] M. C. Bento, O. Bertolami and A. A. Sen, Phys. Rev. D **66**, 043507 (2002) [arXiv:gr-qc/0202064].
- [26] A. Y. Kamenshchik, U. Moschella and V. Pasquier, Phys. Lett. B **511**, 265 (2001) [arXiv:gr-qc/0103004]; N. Bilic, G. B. Tupper and R. D. Viollier, Phys. Lett. B **535**, 17 (2002) [arXiv:astro-ph/0111325].
- [27] A. Dev, D. Jain and J. S. Alcaniz, Phys. Rev. D **67**, 023515 (2003) [arXiv:astro-ph/0209379]; V. Gorini, A. Kamenshchik and U. Moschella, Phys. Rev. D **67**, 063509 (2003) [arXiv:astro-ph/0209395]; R. Bean and O. Dore, Phys. Rev. D **68**, 023515 (2003) [arXiv:astro-ph/0301308]; T. Multamaki, M. Manera and E. Gaztanaga, Phys. Rev. D **69**, 023004 (2004) [arXiv:astro-ph/0307533].
- [28] M. Bordemann and J. Hoppe, Phys. Lett. B **317**, 315 (1993) [arXiv:hep-th/9307036]; N. Bilic, G. B. Tupper and R. D. Viollier, Phys. Lett. B **535**, 17 (2002) [arXiv:astro-ph/0111325].

- [29] J. C. Fabris, S. V. B. Goncalves and P. E. d. Souza, arXiv:astro-ph/0207430.
- [30] R. R. Caldwell, Phys. Lett. B **545**, 23 (2002) [arXiv:astro-ph/9908168].
- [31] L. Parker and A. Raval, Phys. Rev. Lett. **86**, 749 (2001).
- [32] C. Csaki, N. Kaloper and J. Terning, arXiv:astro-ph/0507148.
- [33] V. Sahni and Y. Shtanov, JCAP **0311**, 014 (2003) [arXiv:astro-ph/0202346]; A. Lue and G. D. Starkman, Phys. Rev. D **70**, 101501 (2004) [arXiv:astro-ph/0408246]; C. Csaki, N. Kaloper and J. Terning, Annals Phys. **317**, 410 (2005) [arXiv:astro-ph/0409596].
- [34] B. Feng, M. Li, Y. S. Piao and X. Zhang, arXiv:astro-ph/0407432; G. Barenboim, O. Mena and C. Quigg, Phys. Rev. D **71**, 063533 (2005) [arXiv:astro-ph/0412010].
- [35] G. Barenboim and J. D. Lykken, arXiv:astro-ph/0504090.
- [36] P. Q. Hung, arXiv:hep-ph/0010126; P. Gu, X. Wang and X. Zhang, Phys. Rev. D **68**, 087301 (2003) [arXiv:hep-ph/0307148]; R. Fardon, A. E. Nelson and N. Weiner, arXiv:astro-ph/0309800.
- [37] S. Capozziello, V. F. Cardone, E. Elizalde, S. Nojiri and S. D. Odintsov, arXiv:astro-ph/0508350; V. F. Cardone, C. Tortora, A. Troisi and S. Capozziello, arXiv:astro-ph/0511528.
- [38] P. Astier *et al.*, arXiv:astro-ph/0510447.
- [39] S. Nesseris and L. Perivolaropoulos, arXiv:astro-ph/0511040.
- [40] Y. Wang, Astrophys. J. **536**, 531 (2000) [arXiv:astro-ph/9907405]; Y. Wang and P. Mukherjee, Astrophys. J. **606**, 654 (2004) [arXiv:astro-ph/0312192].
- [41] U. Seljak *et al.*, Phys. Rev. D **71**, 103515 (2005) [arXiv:astro-ph/0407372].
- [42] P. Mukherjee, D. Parkinson, P. S. Corasaniti, A. R. Liddle and M. Kunz, arXiv:astro-ph/0512484.